# Influence of Sigma-Phase Formation on the Localized Corrosion Behavior of a Duplex Stainless Steel

*K.N. Adhe, V. Kain, K. Madangopal, and H.S. Gadiyar*

**Because of their austenitic-ferritic microstructures, duplex stainless steels offer a good combination of mechanical and corrosion resistance properties. However, heat treatments can lower the mechanical strength of these stainless steels as well as render them susceptible to intergranular corrosion (IGC) and pitting corrosion. In this study, a low-carbon (0.02%) duplex stainless steel is subjected to various heat treatments at 450 to 950 °C for 30 min to 10 h. The heat-treated samples then undergo ASTM IGC and pitting corrosion tests, and the results are correlated with the microstructures obtained after each heat treatment. In the absence of $Cr_{23}C_6$ precipitation, σ-phase precipitates render this duplex stainless steel susceptible to IGC and pitting corrosion. Even submicroscopic σ-phase precipitates are deleterious for IGC resistance. Longer-duration heat treatments (at 750 to 850 °C) induce chromium diffusion to replenish the chromium-depleted regions around the σ-phase precipitates and improve IGC resistance; pitting resistance, however, is not fully restored. Various mechanisms of σ-phase formation are discussed to show that regions adjacent to σ-phase are depleted of chromium and molybdenum. The effect of chemical composition (pitting resistance equivalent) on the pitting resistance of various stainless steels is also noted.**

**Keywords**
anodic polarization, duplex stainless steel, intergranular corrosion, pitting corrosion, sigma phase

## 1. Introduction

THE TWO-PHASE ferritic-austenitic microstructure of duplex stainless steels (DSS) imbues them with properties generally unattainable with either austenitic or ferritic stainless steels. Compared to the popular varieties of austenitic stainless steels, DSS offer higher mechanical strength, superior resistance to corrosion, good toughness, weldability, machinability, and cost savings due to their lower nickel content (Ref 1-3). It has been reported (Ref 4) that the mechanical properties of some DSS can exceed those of austenitic stainless steels at operating temperatures of –50 to 250 °C. The use of DSS below –50 °C and above 250 °C makes the ferrite phase susceptible to brittleness. However, DSS are becoming popular in certain environments where austenitic stainless steels exhibit susceptibility to localized corrosion and stress-corrosion cracking (SCC). The main advantages of DSS are in chloride-ion environments; because of their excellent resistance to pitting corrosion and SCC, a number of these types of steels are in use in the marine, petrochemical, oil and gas, chemical, and desalination industries (Ref 1-4).

The susceptibility of austenitic stainless steels to intergranular corrosion (IGC) is attributed to precipitation of $Cr_{23}C_6$ (Ref 5-7) at grain boundaries (upon exposure at 500 to 800 °C), leading to depletion of chromium to a level of less than 12% in regions adjacent to grain boundaries. The same mechanism of sensitization applies to high-carbon DSS (Ref 7). However, some types of DSS contain very low levels of carbon (<0.02%), as well as low levels of nickel (4 to 7%), which does not favor precipitation of $Cr_{23}C_6$ (Ref 4, 8). The presence of molybdenum also helps to delay the precipitation of $Cr_{23}C_6$. Even then, certain heat treatments render DSS susceptible to IGC (Ref 4, 7-9). This paper discusses the mechanism of IGC in a DSS in terms of precipitation of phases other than chromium carbide.

Chromium and molybdenum (Ref 10, 11) contribute to pitting corrosion resistance of stainless steels by providing a protective passive film on the surface. Nitrogen (Ref 12) also helps to increase pitting resistance, although by a different mechanism. Pitting resistance equivalent (PRE) is now commonly used to compare the pitting resistance of various stainless steels [PRE = wt%Cr + 3.3(wt%Mo) + 16(wt%N)] (Ref 4, 13). However, PRE can only be used to assess the pitting resistance of well-annealed materials. Precipitation of various phases due to welding or heat treatments, for example, would adversely affect the pitting resistance of a material (Ref 4, 14, 15). Certain phases can be sites for preferential initiation of pits (Ref 16, 17), whereas others can cause depletion of chromium, nitrogen, and molybdenum (Ref 7, 9, 18) to initiate pits in the depletion zones. Sigma phase has been reported to most adversely affect the mechanical properties as well as the corrosion resistance of DSS (Ref 4, 14, 15, 17, 19-22). This study correlates the precipitation of σ-phase to the pitting corrosion susceptibility of a DSS in chloride-ion environments.

## 2. Experiment and Results

### 2.1 *Heat Treatments and Microstructures*

The DSS used in the study had a chemical composition of Fe-26.0Cr-5.5Ni-2.35Mo-0.8Mn-0.45Si-1.7Cu-0.02C-0.17N (weight percent). Seamless tubes were sectioned in half along the longitudinal direction and flattened by passing through a rolling mill. Rectangular samples (15 by 10 by 1.5 mm) were cut from these strips and sealed in silica tubes under helium atmosphere. They were subjected to a solution annealing heat treatment at 1050 °C for 30 min and then water quenched. A number of solution-annealed samples were subsequently heat treated in the range of 450 to 950 °C at intervals of 100 °C for

**K.N. Adhe, V. Kain, K. Madangopal,** and **H.S. Gadiyar,** Metallurgy Division, Bhabha Atomic Research Centre, Trombay, Bombay 400 085, India.

30 min, followed by water quenching. Another set of solution-annealed samples was heat treated at 550 to 850 °C for periods of 5 and 10 h, then water quenched.

The longitudinal sections of all samples were metallographically prepared. The final steps were diamond finishing and electroetching in a solution of 40% KOH at 5 V for 10 s. The microstructure of a solution-annealed sample is shown in Fig. 1, and that of a sample heat treated at 750 °C for 30 min is shown in Fig. 2. The microstructure of a sample heat treated for 10 h at 750 °C is shown in Fig. 3. Note that the solution-annealed sample shows the typical austenite-ferrite structure of a DSS. Samples heat treated at 750°C for 30 min exhibit a similar structure. No σ-phase could be observed in such samples, but those heated for 10 h contained large quantities of σ-phase—seen as a bluish phase under the optical microscope and as blurred patches in Fig. 3.

### 2.2 *X-Ray Diffraction and TEM Studies*

To quantify the ferrite and austenite phases in various heat-treated samples, x-ray diffraction (XRD) analyses were carried out on the solution-annealed sample and all heat-treated samples. Cu-$K_\alpha$ (filtered) radiation was used for XRD, and peak intensity ratios were used to quantify various phases. The solution-annealed sample contained 60% ferrite and 40% austenite. Various samples heat treated in the temperature range of 450 to 950 °C for 30 min and 10 h showed little variation in the ferrite/austenite ratios. The variation in ferrite content was less than 10%.

Samples heat treated at 450 to 850 °C for 30 min and 10 h were mechanically thinned and then prepared for transmission electron microscopy (TEM) examination by jet thinning in methanol + nitric acid solution. For samples heat treated at 450 to 850 °C for 30 min, no secondary precipitates were observed. Samples heat treated at 750 and 850 °C for 10 h revealed bulky precipitates in place of ferrite phase and were indexed to be σ-phase. Representative bright-field images and the selected-area diffraction (SAD) pattern of the phase are shown in Fig. 4. However, no carbides or nitrides were observed during TEM studies.

### 2.3 *Intergranular Corrosion Test*

The ASTM A 262, practice B, test (Ref 23) was used to evaluate the susceptibility of the material to IGC. Per the practice specifications, samples were exposed to a boiling solution of 50% $Fe_2(SO_4)_3$ + 2.5% $H_2SO_4$ solution for 120 h. Weight loss then was measured. The solution-annealed sample, samples heat treated at 450 to 850 °C for 30 min, and samples heat treated at 650 and 750 °C for 5 and 10 h were

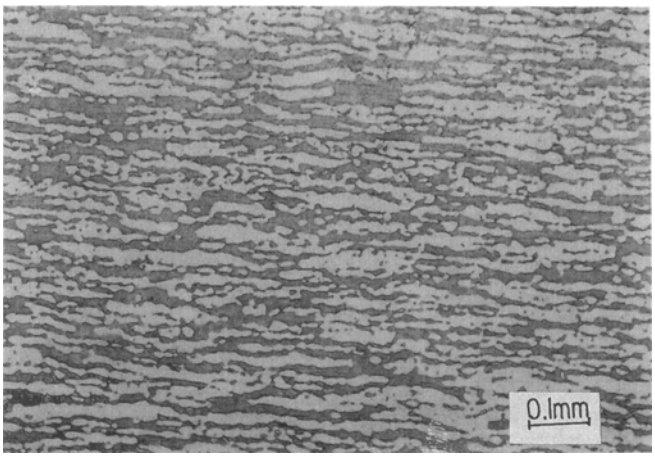


**Fig. 1** Photomicrograph of a DSS sample solution annealed at 1050 °C for 30 min and water quenched

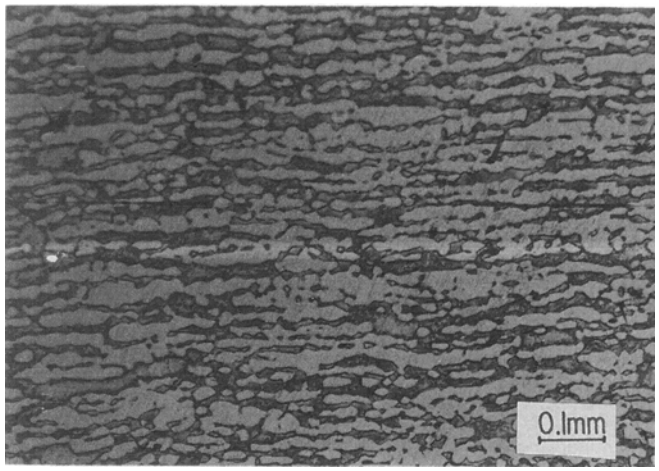


**Fig. 2** Photomicrograph showing a typical microstructure of a DSS sample subjected to 750 °C for 30 min

**Table 1 Results of IGC test for samples heat treated for 30 min at 450 to 950 °C**

| Temperature, °C | Corrosion rate | |
|---|---|---|
| | mpy | mm/year |
| As received | 17.3 | 0.44 |
| 450 | 15.0 | 0.38 |
| 550 | 32.9 | 0.84 |
| 650 | 121.9 | 3.10 |
| 750 | 135.0 | 3.43 |
| 850 | 13.8 | 0.35 |
| 950 | 15.8 | 0.40 |

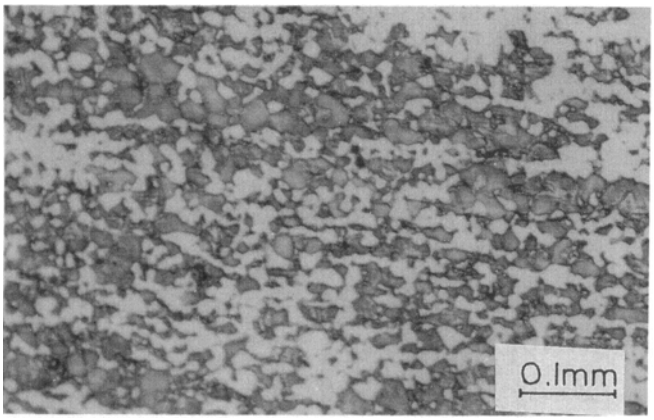


**Fig. 3** Photomicrograph showing a typical microstructure of a DSS sample with σ-phase, subjected to 750 °C for 10 h

tested in the same manner. The measured corrosion rates are listed in Tables 1 and 2.

### 2.4 *Pitting Corrosion Tests*

To assess the effect of chemical composition on pitting behavior, samples of types 304 and 316 LN stainless steel and the DSS (all in the solution-annealed condition) were exposed to 6% $FeCl_3$ solution at room temperature (as per ASTM G 48) (Ref 24) for 24 h. Another set of samples was similarly tested at 50 °C for 24 h. The PRE parameter and the measured corrosion rates are listed in Table 3. A 24 h pitting test in 10% $FeCl_3$ solution was carried out on samples that were heat treated at 550, 650, 750, and 850 °C for 30 min and 10 h. The measured corrosion rates are listed in Table 4.

**Table 2 Results of IGC test for samples heat treated at 650 to 850 °C for various times**

| Temperature, °C | Corrosion rate, mpy (mm/year) | | |
|---|---|---|---|
| | 30 min | 5 h | 10 h |
| 650 | 121.9 (3.10) | 750.5 (19.10) | 210.3 (5.34) |
| 750 | 135.0 (3.43) | 310.2 (7.88) | 75.8 (1.93) |
| 850 | 13.8 (0.35) | 149.4 (3.79) | 44.5 (1.13) |

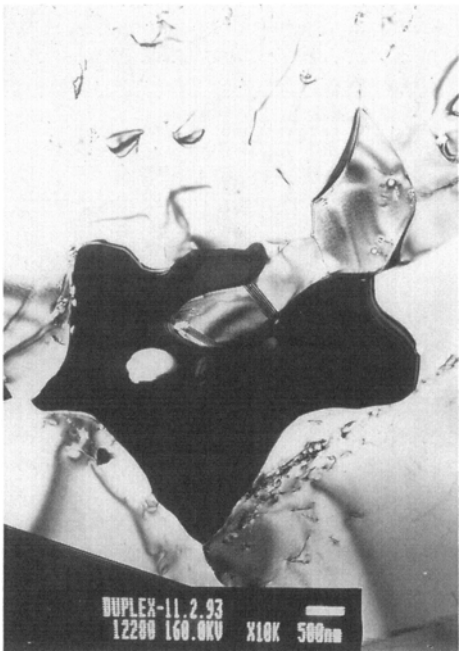


(a)


(b)


(c)

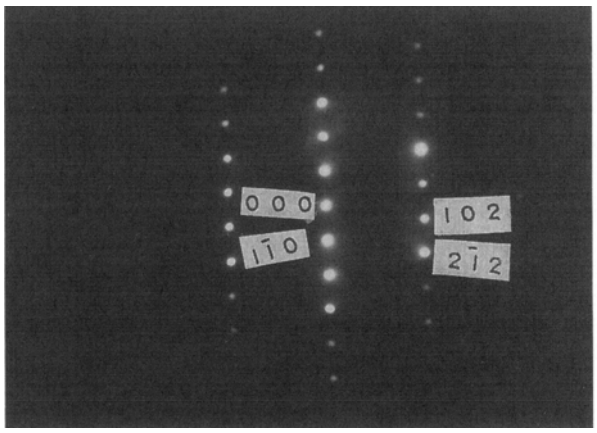


(d)

**Fig. 4** Bright-field images (a to c) and SAD pattern (d) of σ-phase in a DSS sample heat treated at 750 °C for 10 h

Pitting corrosion susceptibility was also evaluated by anodic polarization experiments in 1 *N* HCl solution at room temperature (deaerated by passing argon gas 1 h before and during the test). Each sample was mounted in cold-setting resin after electrical contact was provided on the back face of the sample. The sample surface was metallographically prepared to a diamond finish. Potentials were scanned from −400 to +1100 mV (SCE) at a scan rate of 20 mV/min. Anodic polarization curves are plotted in Fig. 5 for samples heat treated at 650, 750, and 850 °C for 30 min and in Fig. 6 for samples heat treated at the same temperatures for 10 h. The pitting potentials, $E_{pit}$, as derived from these experiments, are tabulated in the graphs.

## 3. Discussion

The DSS used for this study contained 60% ferrite and 40% austenite in its solution-annealed condition. This is clear from its microstructure (Fig. 1) and from the TEM studies, which revealed no other phase. Subsequent heat treatments in the temperature range of 450 to 950 °C for periods ranging from 30 min to 10 h showed no significant variation in the ferrite-austenite ratio as assessed by XRD. This is in conformance with studies (Ref 25) that reported ferrite contents due to heat treatments above 1050 °C and lesser variation of ferrite contents due to heat treatments below 1050 °C.

It has been reported that the ferrite phase is unstable at temperatures above 450 to 550 °C and can decompose to give σ-phase and secondary austenite. There may be three distinct mechanisms (Ref 4) by which the secondary austenite forms from the ferrite phase. In the first, the eutectoid reaction, $\delta \rightarrow \sigma + \gamma_2$, is facilitated by rapid diffusion along the δ/γ boundaries and results in a typical eutectoid structure of σ-phase and austenite in prior-ferrite grains. It is reported to typically occur in the temperature range of 700 to 900 °C. The σ-phase has a tetragonal structure and is rich in chromium, molybdenum, and silicon (Ref 26), and the secondary austenite (surrounding the σ-phase) becomes depleted of these elements.

According to the second reported mechanism, below about 650 °C ferrite in a DSS transforms to austenite via a mechanism that is similar to martensitic transformation. This austenite transforms isothermally and shows no difference in composition compared with the ferritic host matrix, indicating a diffusionless transformation. At temperatures above 650 °C, according to the third mechanism, diffusion is more predominant and austenite forms in a Widmanstätten morphology. There is a difference in composition between the austenite and the ferrite matrix due to diffusion.

Intergranular corrosion rates (Table 1) for the solution-annealed sample and the sample heated at 450 °C for 30 min are comparable; this indicates that there is no precipitation of σ-phase due to that heat treatment. However, the corrosion rate increases with increasing heat treatment temperature up to 650 °C for 30 min. Although no precipitation of carbides or σ-phase could be observed in optical microscopic and TEM studies, it is known that nucleation of σ-phase starts at the α/γ boundaries as submicroscopic σ. This submicroscopic σ (Ref 27) leads to formation of associated secondary austenite (first mechanism) or formation of secondary austenite (third mechanism), providing regions depleted of chromium and molybdenum. These regions are susceptible to attack in corrosive solutions (e.g., ASTM A 262, practice C, and 25% $H_2SO_4$ at 25 °C [Ref 28]) and are manifested by a higher degree of attack in the practice B test. However, samples heat treated at 850 and 950 °C for 30 min do not show much higher corrosion rates than the annealed sample, indicating the absence of chromium- and molybdenum-depleted regions (and σ-phase).

The corrosion rates of samples heat treated at 650 and 750 °C for 10 h (Table 2) are higher than for the solution-annealed sample but lower than for samples heat treated for 5 h. This indicates that susceptibility to IGC increases as heat treatment is carried out for more than 30 min, reaches a maximum value, and then reduces when the sample is heated for 10 h. This trend is followed by precipitation kinetics and σ-phase (and secondary austenite). As heat treatment time is increased from 30 min to 5 h, more and more σ-phase is formed and thus more secondary austenite adjacent to it, which is depleted of chromium and molybdenum. These depleted regions are attacked in the ASTM A 262, practice B, environment.

However, at these temperature, diffusion also comes into play. Fast diffusion rates in the ferrite matrix allow for fast replenishment of chromium and molybdenum (Ref 29) to these depleted regions (secondary austenite). Heat treatments for 10 h have already replenished chromium and molybdenum to the depleted regions to a large extent, and the effect on lowering of corrosion rates is clearly evident. Compared to fast replenishment in DSS (or ferritic stainless steels), austenitic stainless steels require much longer time for replenishment: 15 days at 750 °C and 5 days at 800 °C for type 304 (Ref 30) containing 0.06% C.

**Table 3 Pitting resistance equivalent and pitting corrosion rates measured in 6% $FeCl_3$ solution at room temperature and 50 °C**

| Stainless steel | PRE | Temperature, °C | Corrosion rate | |
|---|---|---|---|---|
| | | | mdd | mm/year |
| Type 304 | 18.00 | RT | 508.8(a) | 1.48(a) |
| | | 50 | 5460.6(b) | 24.96(b) |
| Type 316 LN | 28.44 | RT | 21.4(c) | 0.09(c) |
| | | 50 | 1055.9(d) | 4.85(d) |
| Duplex | 36.48 | RT | 1.1(c) | 0.005(c) |
| | | 50 | 350.2(e) | 1.60(e) |

(a) Number of pits on all surfaces. (b) Heavy pitting corrosion. (c) Uniform corrosion only. (d) Mainly heavy general corrosion; few pits on the edges. (e) Generally uniform corrosion; few pits on the edges only

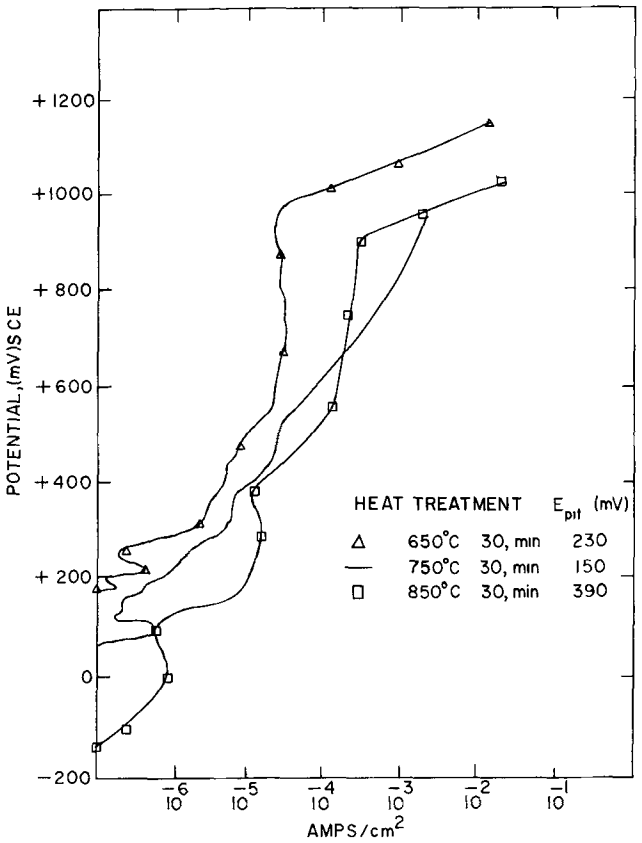


**Fig. 5** Anodic polarization curves for a DSS sample heat treated for 30 min at 650 to 850 °C in 1 *N* HCl (deareated) at room temperature

At 850 °C, the sample exposed to the 30 min heat treatment shows the same corrosion rate as the sample in the simple solution-annealed condition. However, sample heat treated for 10 h shows higher corrosion rates. Microstructural studies of etched samples (850 °C, 10 h) revealed large proportions of σ-phase. This implies that at 850 °C, 10 h, the σ-phase formation reaction is nearly complete and that faster replenishment of chromium and molybdenum has also taken place.

It can be inferred from these studies that submicroscopic σ-phase formation at α/γ boundaries is detrimental for IGC resistance (in the practice B test), as severely depleted secondary austenite would be present at the phase boundaries. Longer-duration heat treatments result in bulky σ-phase formation and larger secondary austenite, but also provide for fast replenishment of chromium and molybdenum due to faster diffusion rates through the ferrite phase. This somewhat increases the resistance to IGC (Ref 9), and if proper heat treatments are used the corrosion rates in practice B can be brought to very low (acceptable) values.

The results of the pitting resistance tests in 6% $FeCl_3$ solution (Table 3) are supported by reported studies (Ref 4) where the PRE has been correlated to the critical pitting temperature in the ASTM G 48 test. The effect of chemical composition (particularly chromium and molybdenum) on pitting resistance is evident from the lowest pitting resistance of type 304 stainless steel (PRE = 18.0) at room temperature and 50 °C. Type 316 LN (PRE = 28.5) shows good pitting resistance at room

**Table 4 Pitting corrosion rates measured in 10% $FeCl_3$ solution at room temperature for variously heat-treated DSS**

| Heat treatment temperature, °C | Heat treatment duration | Corrosion rate | |
|---|---|---|---|
| | | mpy | mm/year |
| 550 | 30 min | 0.17(a) | 0.004(a) |
| | 10 h | 28.4(a) | 0.72(a) |
| 650 | 30 min | 1.0(a) | 0.02(a) |
| | 10 h | 282(b) | 7.16(b) |
| 750 | 30 min | 264(b) | 6.70(b) |
| | 10 h | 522(b) | 13.26(b) |
| 850 | 30 min | 33.4(c) | 0.85(c) |
| | 10 h | 55.7(a) | 1.42(a) |

(a) No pits observed. (b) Severe pitting corrosion. (c) General corrosion only

temperature, but starts to pit by 50 °C. The DSS used in the study (PRE = 36.5) shows the lowest corrosion rate (no pitting) at both room temperature and 50 °C. At 50 °C small pits were observed at one location on the edges of the sample, but the other surfaces were unaffected. This shows that DSS has much superior pitting resistance compared to commonly used austenitic stainless steels. Duplex stainless steels with markedly higher resistance to pitting corrosion in chloride-ion environments (critical pitting temperature, in the G 48 test, as high as 80 °C) are also available. These steels, classified as super DSS, have PRE values greater than 40. Their resistance is achieved by increasing the compositional amounts of chromium (typically 25%), molybdenum (up to 4%), and nitrogen (as high as 0.3%) (Ref 4, 21).

However, heat treatments that result in precipitation of σ-phase (and regions depleted of chromium and molybdenum) render the DSS susceptible to pitting in $FeCl_3$ even at room temperature (Ref 14, 15, 22). Table 4 shows that the sample heat treated at 750 °C for 30 min exhibited a maximum corrosion rate in 10% $FeCl_3$ at room temperature, whereas samples heat treated at 650 and 850 °C showed much lower corrosion rates (better resistance to pitting). Samples heat treated for 10 h at 650 and 750 °C, however, showed much higher corrosion rates and pitting than those heated for 30 min. This is because the pitting test employed is very vigorous (10% $FeCl_3$), and the larger regions of secondary austenite are available for samples heated for 10 h (although replenished, but not to the full extent). Therefore, these regions are suitable sites for pit nucleation. The effect of replenishment becomes clear in the potentiodynamic experiments (Fig. 5 and 6), which reveal that the longer-duration (10 h) heat treatments at 650 and 750 °C (where replenishment of chromium and molybdenum is still incomplete) result in increased critical current density, $i_c$ (two orders of magnitude more than for samples heated at 450 °C) and higher passivation currents, $i_p$ (one order of magnitude higher than for samples heated at 450 °C). However, heat treatment at 850 °C for 10 h (where replenishment is mostly complete) brings down the $i_c$ and $i_p$ close to the corresponding values for the sample heated at 450 °C for 30 min. Similarly, the pitting potentials, $E_{pit}$, are also brought down by the 10 h heat treatments.

It may be further noted that $E_{pit}$ is minimum (maximum pitting susceptibility) for the sample heated at 750 for 30 min. This correlates well with the results of the pitting corrosion test

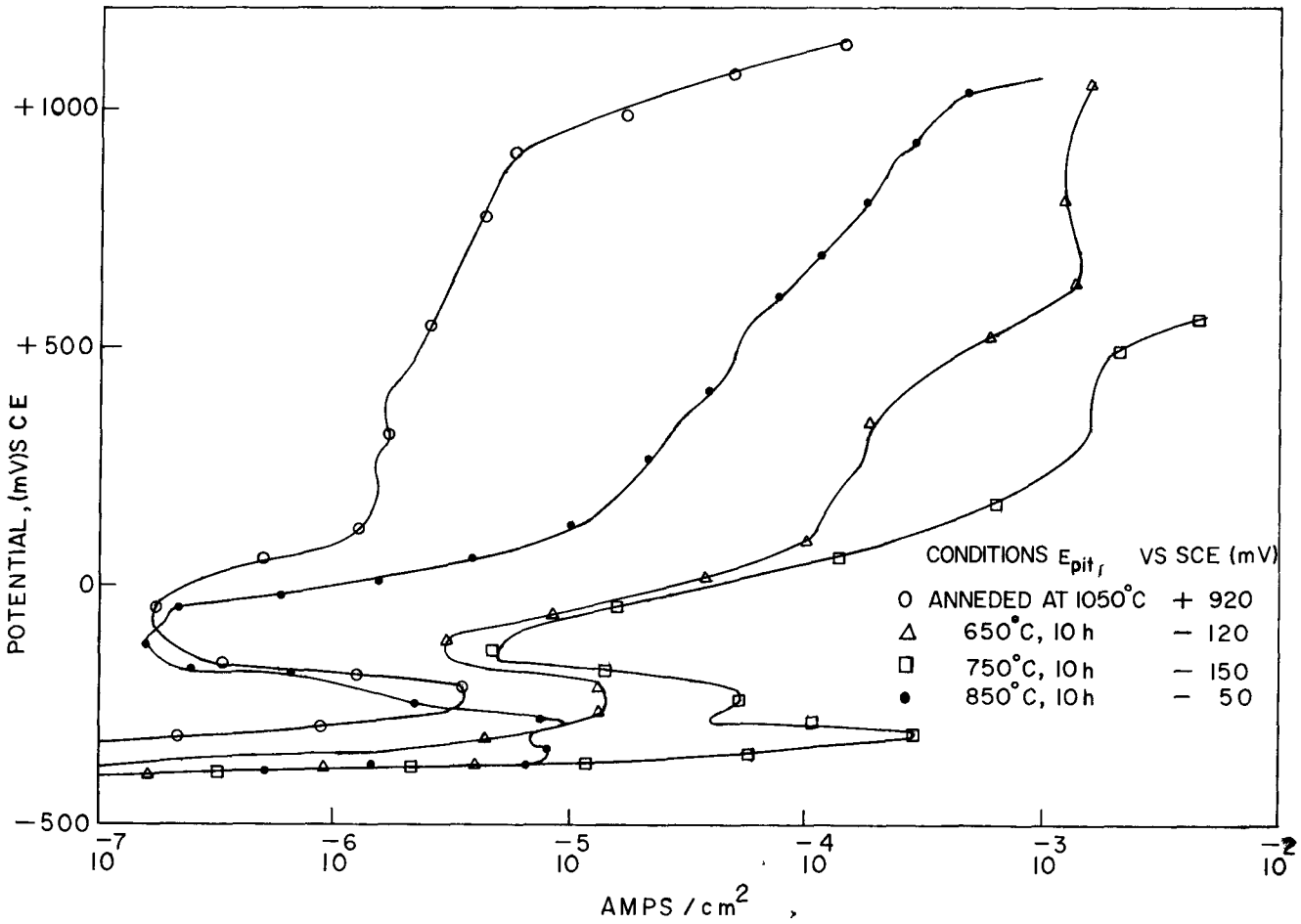


**Fig. 6** Anodic polarization curves for a DSS sample heat treated for 10 h at 650 to 850 °C in 1 *N* HCl (deareated) at room temperature

(Table 4) and the IGC test results (which show maximum susceptibility for the sample heated at 750 for 30 min, Table 1). It is clear from these results that to restore pitting corrosion resistance, higher levels of replenishment of chromium and molybdenum are required than are needed to restore IGC resistance.

## 4. Conclusions

The following inferences can be drawn from the present study:

- Submicroscopic σ-phase is more deleterious with regard to IGC than the bulky σ-phase, as short-duration heat treatments also cause increased IGC.
- The depletion of chromium and molybdenum in regions adjacent to the σ-phase (i.e., in secondary austenite) causes IGC and pitting attack.
- Longer-duration heat treatments at 650 to 750 °C improve resistance to IGC due to replenishment of chromium and molybdenum.
- Higher levels of chromium, molybdenum, and nitrogen in DSS provide superior pitting resistance in the annealed conditions, but precipitation reactions due to heat treatments render DSS susceptible to pitting.
- Longer-duration heat treatments at 750 °C restore IGC resistance, but are not sufficient to restore the pitting resistance of DSS in aggressive chloride-ion environments (10% $FeCl_3$). In electrochemical experiments in 1 *N* HCl, $E_{pit}$ values are lowered by longer-duration heat treatments. However, other parameters (e.g., $i_c$ and $i_p$) are restored by heat treatments that result in still higher levels of replenishment (e.g., 850 °C for 10 h).

### Acknowledgment

The authors are thankful to Dr. S. Banerjee, Head, Metallurgy Division, for his keen interest in our work and permission to publish this paper.

### References

1. G. Bergland and P. Wilhelmsson, Fabrication and Practical Experience of Duplex Stainless Steels, *Mater. Des.*, Vol 10 (No. 1), 1989, p 23-28
2. R. Longneberg and J. Johnson, Stainless Steels in the '90s, *Mater. Des.*, Vol 10 (No. 3), 1989, p 144-152
3. H. Solomon and T. Devine, Jr., Tale of Two Phases, *Duplex Stainless Steels*, R.A. Lula, Ed., American Society for Metals, 1983, p 693-756
4. J.O. Nilsson, Superduplex Stainless Steels, *Mater. Sci. Technol.*, Vol 8, 1992, p 685-700

5. R.L. Cowan and C.S. Tedman, Intergranular Corrosion for Iron-Nickel-Chromium Alloys, *Advances in Corrosion Science and Technology,* Vol 13, M.G. Fontana and R.W. Staehle, Ed., Plenum Press, 1973, p 293-400
6. C.S. Tedman, D.A. Vermilyea, and J.H. Rosolowski, Intergranular Corrosion of Austenitic Stainless Steels, *Electrochem. Soc.,* Vol 118 (No. 2), 1971, p 192-202
7. T.M. Devine, Mechanism of Intergranular Corrosion and Pitting Corrosion of Austenitic and Duplex 308 Stainless Steel, *J. Electrochem. Soc.,* Vol 126 (No. 3), 1979, p 374-385
8. T.M. Devine, Influence of Carbon Content and Ferrite Morphology on the Sensitization of Duplex Stainless Steel, *Metall. Trans.,* Vol 11A, 1980, p 791-800
9. K. Ravindranath and S.N. Malhotra, The Influence of Aging on the Intergranular Corrosion of 22 Chromium-5 Nickel Duplex Stainless Steel, *Corros. Sci.,* Vol 37 (No. 1), 1994, p 121-132
10. J.R. Galvele, J.B. Lumsden, and R.W. Staehle, Effect of Molybdenum on the Pitting Potential of High Purity 18% Cr Stainless Ferritic Steel, *J. Electrochem. Soc.,* Vol 125 (No. 8), 1978, p 1204-1208
11. R.J. Brigham, Pitting and Crevice Corrosion Resistance of Commercial 18%Cr Stainless Steel, *Mater. Perform.,* Vol 13 (No. 11), 1974, p 29-31
12. G.C. Palit, V. Kain, and H.S. Gadiyar, Electrochemical Investigations of Pitting Corrosion in Nitrogen Bearing Type 316 LN Stainless Steel, *Corrosion,* Vol 49 (No. 12), 1993, p 977-991
13. J.E. Truman, *Met. Mater. Technol.,* Jan 1980, p 15
14. J.H. Potgieter, Influence of σ Phase on General and Pitting Corrosion Resistance of SAF 2205 Duplex Stainless Steel, *Br. Corros. J.,* Vol 27 (No. 3), 1992, p 219-223
15. J.H. Potgieter, Discussion on Influence of σ Phase on General and Pitting Corrosion Resistance of SAF 2205 Duplex Stainless Steel, *Br. Corros. J.,* Vol 27 (No. 4), 1992, p 319-320
16. V. Kain, G.C Palit, S.S. Chouthai, and H.S. Gadiyar, Effect of Heat Treatment on the Critical Pitting Potential of SS 304 in 0.01 *N* NaCl, *J. Electrochem. Soc. India,* Vol 38 (No 1), 1989, p 50-54
17. H.D. Solomon and T.M. Devine, *Influence of Microstructure on the Mechanical Properties and Localized Corrosion of a Duplex Stainless Steel,* STP 672, ASTM, 1979, p 430-461
18. Y. Maehara, Y. Ohmori, and T. Kunitake, *Met. Technol.,* Vol 10, 1983, p 296-303
19. M.E. Wilms, V.J. Gadgil, J.M. Krougmen, and B.H. Kolster, The Effect of σ Phase Precipitation at 800 °C on the Mechanical Properties of a High Alloyed Duplex Stainless Steel, *Mater. High Temp.,* Vol 9 (No. 3), 1991, p 160-166
20. M.E. Wilms, V.J. Gadgil, J.M. Krougmen, and F.A. Ijsseling, The Effect of σ Phase Precipitation at 800 °C on the Corrosion Resistance in Sea Water of a High Alloyed Duplex Stainless Steel, *Corros. Sci.,* Vol 36 (No. 5), 1994, p 871-881
21. A.J. Sedricks, New Stainless Steels for Sea Water Service, *Corrosion,* Vol 45 (No. 6), 1989, p 510-518
22. T.M. Devine and B.J. Drummand, Use of Accelerated Intergranular Tests and Pitting Corrosion Tests to Detect Sensitization and Susceptibility to Intergranular Stress Corrosion Cracking in High Temperature Water of Duplex 308 Stainless Steel, *Corrosion,* Vol 37 (No. 2), 1981, p 104-115
23. "Recommended Practice for Detecting Susceptibility to Intergranular Attack in Stainless Steels, A 262, *Annual Book of ASTM Standards,* ASTM, 1989, p 1-18
24. "Test for Pitting and Crevice Corrosion Resistance of Stainless Steels and Related Alloys by the Use of Ferric Chloride Solution," G 48, *Annual Book of ASTM Standards,* ASTM, 1989
25. H.D. Solomon, Age Hardening in a Duplex Stainless Steel, *Duplex Stainless Steels,* R.A. Lula, Ed., American Society for Metals, 1983, p 41-70
26. Y. Maehara, Y. Ohmori, J. Murayama, N. Fujino, and T. Kunitake, *Mater. Sci.,* Vol 17, 1983, p 541-547
27. M.A. Streicher, General and Intergranular Corrosion of Austenitic Stainless Steels in Acids, *J. Electrochem. Soc.,* Vol 106, 1959, p 161-180
28. D. Warren, Effect of Sigma Phase vs Chromium Carbides on the Intergranular Corrosion of Type 316 and 316 L Stainless Steels, Parts I and II, *Corrosion,* Vol 15 (No. 4 and 5), 1959, p 213t-232t
29. P. Sury, *Mater. Chem.,* Vol 1, 1976, p 151
30. K.N. Adhe, V. Kain, S.S. Chouthai, and H.S. Gadiyar, Effect of Time and Temperature of Desensitization on the Chromium Depleted Region in AISI 304 Stainless Steel, *Indian J. Technol.,* Vol 28, 1990, p 139-142